Alternative Incorporation Procedure of Quantum Dots in Polymer Microspheres

Richard Karel Čapek,[†] Michael Weber,[‡] and Alexander Eychmüller*,[§]

[†]*Physics and Chemistry of Nanostructures, Ghent University, Krijgslaan 281-S12, 9000 Ghent, Belgium,*
[‡]*Pavel Tomancak lab, Max Planck Institute of Molecular Cell Biology and Genetics, Pfotenhauerstrasse 108,*
01307 Dresden, Germany, and [§]*Physical Chemistry, TU Dresden, Bergstr. 66b, 01062 Dresden, Germany*

Received April 11, 2010. Revised Manuscript Received June 7, 2010

Quantum dot doped microspheres possess a broad range of possible applications from photonics to biolabeling. These doped microspheres can be prepared by many different approaches. Here we will focus on a strategy, where first prepared polymer microspheres are subsequently doped with semiconductor nanoparticles. The described procedure enables us to gain directly aqueous suspensions of quantum dot doped polymer microspheres which can be used to prepare high quality artificial opals by self-assembly procedures. The properties of these quantum dot doped polymer microspheres and the artificial opals made thereof will be discussed.

Introduction

The combination of semiconductor nanoparticles (QDs) with polymer microspheres (PMCs) possess potential in biological[1,2] and photonic crystal applications.[3−6]

One of the advantages of the combination of these materials is that their optical properties can be adjusted to each other (each, the absorption and emission properties of QDs and the photonic properties of PMCs depending on their particular size), meaning that a facile adoption of a combined material can be performed with regard to a certain task.[7−9]

Different procedures are known to link nanoparticles to PMCs: among others the attachment of QDs by "layer-by-layer" assembly to microspheres, incorporation of QDs in PMCs during the synthesis of the PMCs, two step procedures where QDs are incopereted in polymer nanospheres by miniemulsion polymerization followed by a core shell polymerization to gain larger PMCs and incorporation procedures of already prepared PMCs with QDs.[1,2,10−15]

An incorporation procedure of already prepared PMCs was presented by Han et. al:[2] cross-linked PMCs (c-PMCs) were swollen in an alcohol/chloroform mixture. Subsequently QDs, dissolved in chloroform, were added and infiltrated the c-PMCs. The suspensions of QD-doped c-PMCs were purified and finally suspensions of c-PMCs were obtained in alcohols.

This procedure allows the loading of c-PMCs with a large number of QDs, but the amount of doped c-PMCs gained is typically low. Furthermore, for biological and self-assembly applications, further processing of the samples is necessary to receive the doped c-PMCs in water.

Here we present an incorporation procedure, where c-PMCs were doped with CdSe/CdS core/shell QDs. The procedure starts from suspensions of c-PMCs in water and gains finally the doped c-PMCs directly in water. The morphological and optical properties of these doped c-PMCs were investigated. Furthermore, the doped c-PMCs prepared according to this approach were used to prepare artificial opals, which morphological and optical properties also were investigated.

Experimental Section

Chemicals. Solvents were mainly purchased from Merck (p.a. grade), tetrahydrofurane (THF) was purchased from Aldrich (p.a.), methylmethacrylate (MMA) and divinylbenzene (DVB) were purchased from Merck (p.s. grade) and trioctylphosphine from Fluka (technical grade). The monomers and trioctylphospine (TOP) were purified by distillation. The monomers were stored at −20 °C and TOP under nitrogen. Potassiumperoxodilsulfate (KPS, Merck, p.a.), trioctylphosphinoxide (TOPO, Merck, > 98%), cadmiumacetate (ChemPur, 99.99%), selenium (ChemPur, 99,99%),

(1) Chan, Y.; Zimmer, J. P.; Stroh, M.; Steckel, J. S.; Jain, R. K.; Bawendi, M. G. *Adv. Mater.* **2004,** *16,* 2092.
(2) Han, M. Y.; Gao, X. H.; Su, J. Z.; Nie, S. *Nat. Biotechnol.* **2001,** *19,* 631.
(3) Romanov, S. G.; Chigrin, C. N.; Sotomayor Torres, C. M.; Gaponik, N.; Eychmüller, A.; Rogach, A. L. Phys. Rev. E **2004,** *69.*
(4) Gaponenko, S. V.; Kapitonov, A. M.; Bogomolov, V. N.; Prokofiev, A. V.; Eychmuller, A.; Rogach, A. L. *JETP Lett.* **1998,** *68,* 142.
(5) Lodahl, P.; van Driel, A. F.; Nikolaev, I. S.; Irman, A.; Overgaag, K.; Vanmaekelbergh, D. L.; Vos, W. L. *Nature* **2004,** *430,* 654.
(6) Gaponik, N.; Eychmüller, A.; Rogach, A. L.; Solovyev, V. G.; Sotomayor Torres, C. M.; Romanov, S. G. *J. Appl. Phys.* **2004,** *95,* 1029.
(7) Brus, L. E. *J. Chem. Phys.* **1984,** *80,* 4403.
(8) Yablonovitch, E. *Phys. Rev. Lett.* **1987,** *58,* 2059.
(9) John, S. *Pys. Rev. Lett.* **1987,** *58,* 2486.
(10) Caruso, F.; Spasova, M.; Saigueirino-Maceira, V.; Liz-Marzan, L. M. *Adv. Mater.* **2001,** *13,* 1090.
(11) Radtchenko, I. L.; Sukhorukov, G. B.; Gaponik, N.; Kornowski, A.; Rogach, A. L.; Mohwald, H. *Adv. Mater.* **2001,** *13,* 1684.
(12) Yang, X. T.; Zhang, Y. *Langmuir* **2004,** *20,* 6071.
(13) Sheng, W. C.; Kim, S.; Lee, J.; Kim, S. W.; Jensen, K.; Bawendi, M. G. *Langmuir* **2006,** *22,* 3782.
(14) Fleischhaker, F.; Zentel, R. *Chem. Mater.* **2005,** *17,* 1346.
(15) Gao, X. H.; Nie, S. M. *Anal. Chem.* **2004,** *76,* 2406.

n-tetradecylphosphonic acid (TDPA, Alfa Aesar, 99%) and hexa-decylamine (HDA, Merck, 99%) were used as received.

Apparatus. Absorption spectra of nanoparticle solutions in chloroform were taken with a Varian Cary 500 conc UV−vis absorption spectrometer. Diffuse reflection spectra of aqueous dispersions of QD doped c-PMCs were taken with an integrating sphere (Labsphere DRA-CA-5500, accessory for a Varian Cary 500 conc UV−vis NIR absorption spectrometer). Emission spectra of QD-solutions were taken with a Jobin Yvon Fluorolog emission spectrometer (spectral resolution: excitation and detection 2 nm). Emission spectra of aqueous dispersions of QD doped c-PMCs were also taken with a Jobin Yvon Fluorolog (spectral resolution: excitation and detection 2 nm), but in a front-face geometry. To reduce scattered light a K-40 band-pass filter was set in the excitation and a GG 495 high-pass filter was set in the detection beam.

Emission spectra of QD-doped artificial opals were taken with a Jobin Fluoromax using an HG 436 63 Bandpassfilter, Carl Zeiss.

Specular reflection spectra were taken with Varian variable angle specular reflection accessory (VASRA, accessory for a Varian 5000 UV−vis/NIR absorption spectrometer). The incident beam was polarized with polarization slides (equipment Varian VASRA). The reflection spectra were normalized versus a silver mirror (Linos).

TEM-images were taken with a high resolution transmission microscope Phillips CM-300. SEM-images of gold coated opals (AGAR sputter coater) were taken with a scanning electron microscope Zeiss DSM 982 Gemini.

Dynamic Light Scattering measurements were performed with a setup of the ALV Langen GmbH.

CdSe/CdS-QD Synthesis. CdSe/CdS-QDs were synthesized similar to the procedure published by Mekis et al.[16]

A mixture of 5 g of HDA and 8 g of TOPO was heated up to 120 °C and kept for 2 h under vacuum. Under nitrogen 0.15 g of TDPA dissolved in 1.5 mL THF were added. The THF was evaporated under vacuum. Under a nitrogen atmosphere 2 mL of a 2 M solution of selenium dissolved in TOP were added. The reaction mixture was heated up to 300 °C and 0.12 g cadmiumacetate dissolved in 3 mL of TOP by were injected. The temperature was reduced to 260 °C and the reaction mixture was allowed to last at 260 °C for 10 min before the temperature was reduced to 120 °C.

To grow the CdS on the core-nanoparticles the nitrogen flow was stopped and 30 mL of H_2S were added in portions of 2 mL every 15 min. After the H_2S addition the temperature was decreased to 100 °C and the reaction mixture was allowed to last at this temperature for one hour. Then the temperature was increased to 120 °C and the H_2S was removed by applying vacuum.

Afterward 0.8 g $CdAc_2$ dissolved in 2 mL TOP and 0.4 g TDPA dissolved in 4 mL of THF were added, and the THF was removed under vacuum. Finally the reaction mixture was stirred at 120° overnight.

The crude product was dissolved in about 500 mL of 90 °C warm toluene. The temperature was reduced to 20 °C, and the precipitate was removed by centrifugation. The obtained solution was checked by UV−vis spectroscopy. This step was repeated until a strongly enhanced absorption for wavelengths below 500 nm was observed in comparison to the previous samples, indicating an impurity of CdS nanoparticles.

Copolymer Microspheres. C-PMCs were prepared by a surfactant free emulsion polymerization.[17] 100 mL of water were placed in a 250 mL tree necked round-bottom flask. Then the water was stirred under a nitrogen flow (stirring speed: 750 rotations/min) for 30 min. The nitrogen flow was stopped and 8.4 mL of MMA and 0.9 or 0.17 mL of DVB (1 or 2% cross-linked spheres, respectively), were added. The temperature was increased to 90 °C (oil bath temperature) and the reaction mixture was allowed to last for 2 h. Five ml of a solution of 1 g of KPS dissolved in 5 mL of water were injected at 90 °C (oil bath temperature). The polymerization reaction was allowed to proceed for another 2 h until it was stopped by opening the flask. To remove not reacted monomer, the reaction mixture was stirred for another 2 h at 90 °C. The crude product was filtered. Then the c-PMCs were separated from the suspension by centrifugation and redispersed in water at least two times. To remove larger agglomerates from the suspension a short centrifugation run was performed, which allowed to separate 5−10% of the product from the suspension.

Infiltration Procedure. In a typical infiltration procedure about 0.25 g of a c-PMC suspension in water (44 wt % polymer for 1% cross-linked c-PMCs and 40.2 wt % polymer for 2% cross-linked c-PMCs) were dispersed in 10 mL of acetone. Then 10 mL of chloroform and 50 μL of water were added, followed by an addition of 1.2 mL of a QD solution in chloroform (OD at $\lambda_{1s-1s} \sim 2$). The infiltration mixture was allowed to last under stirring for 8 h (1% cross-linked spheres) or for or 12 h (2% cross-linked spheres). The reactions were performed in closed flasks to reduce the influence of moisture.

Afterward 20 mL of a 3:1 mixture of methanol and water were added and the majority of the organic solvents were evaporated in less than 5 min under reduced pressure and heating (it has to be remarked, that if the evaporation of the organic solvents is performed slower a separation of the c-PMCs and the QDs, combined with a precipitation of the QDs, occurs). The volume of the residual suspension was reduced to less than 2 mL by evaporation, then 50 mL of water were added and the volume was reduced again by evaporation to less than 2 mL. The obtained doped c-PMCs were separated from the solvent by centrifugation and redispersed in water. This procedure was repeated several times. In a last centrifugation step a small fraction of the polymer was separated to remove agglomerates of c-PMCs.

Preparation of Thin Films of Artificial Opals. Thin opaline films were prepared by a vertical deposition technique at 47 °C and volume fractions of polymer in water of 0.001−0.005.[18,19]

Results and Discussion

Optical Properties of Infiltrated c-PMCs. In Figure 1(a) diffuse reflection spectra of suspensions of QD-doped c-PMCs in water and the absorption spectra of the corresponding QDs in chloroform are shown. The peak wavelength of the first electronic transition (λ_{1s-1s}) for both QD-doped c-PMCs is shifted slightly to shorter wavelengths in comparison to the QDs in chloroform. This effect can be attributed to a partial dissolution of the QDs during the incorporation process. In Figure 1(b) the emission spectra of the mentioned samples are shown. Like the λ_{1s-1s} also the

(16) Mekis, I.; Talapin, D. V.; Kornowski, A.; Haase, M.; Weller, H. *J. Phys. Chem. B* **2003**, *107*, 7454.

(17) Egen, M.; Zentel, R. *Chem. Mater.* **2002**, *14*, 2176.
(18) Dimitrov, A. S.; Nagayama, K. *Langmuir* **1996**, *12*, 1303.
(19) Jiang, P.; Bertone, J. F.; Hwang, K. S.; Colvin, V. L. *Chem. Mater.* **1999**, *11*, 2132.
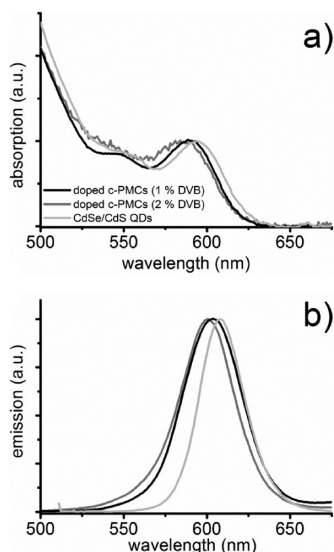
Figure 1. (a) Absorption and (b) emission spectra of QD-doped c-PMCs, dissolved in water, in comparison to the QDs used for doping, dissolved in chloroform.

Figure 2. (a) Confocal microscopy fluorescence images of doped (a) c-PMCs 1% and (c) 2% and confocal microscopy images of doped (b) c-PMCs 1% and (d) c-PMCs 2%.

Figure 3. TEM-image of doped c-PMCs 2%.

emission peak wavelengths are shifted slightly to shorter wavelengths. Furthermore, the emission spectra of the doped c-PMCs are broadened in comparison to the corresponding QDs in chloroform. Because of the difference of the particular measurements, it is not clear whether the observed broadening after infiltration can be attributed to a degradation of the QDs during the incorporation or to the different measurement conditions (e.g., diffuse scattering of the suspensions of doped c-PMCs vs absorption of the clear QD solutions).

To confirm that the luminescence originates from the c-PMCs, confocal microscopy images and confocal microscopy fluorescence images were taken. The c-PMCs, having here a diameter of about 320 nm (determined by dynamic light scattering), appear in the confocal microscopy image as circular diffraction patterns with a diameter of about 1 μm or, for larger arrangements of spheres, as structured areas.

The comparison of the confocal microscopy image of doped c-PMCs (content PDVB 1 wt %; c-PMCs 1%) with the fluorescence image shows, that the luminescence is emitted relatively homogeneous from the areas where c-PMCs are present (Figure 2(a) and (b)). In the case of the doped polymer spheres (with 2 wt % PDVB cross-linked c-PMCs (c-PMCs 2%)) the luminescence appears also only from areas where polymer is present, but aside from a relatively homogeneous luminescence also bright spots are observed. (Figure 2(c) and (d)).

In TEM-images of doped c-PMCs 2% single QDs appear to be distributed in all spheres. Occasionally, agglomerates of QDs within the c-PMCs can be observed (Figure 3). To examine whether the luminescence of the bright spots observed in the confocal fluorescence microscopy images can be related to the agglomerates of QDs in c-PMCs, emission spectra were taken from different sites of a monolayer of QD doped c-PMCs, with a confocal fluorescence microscope (Figure 4(a) and (b)). It turns out, that the emission of the bright spots (spots 1 and 2 in
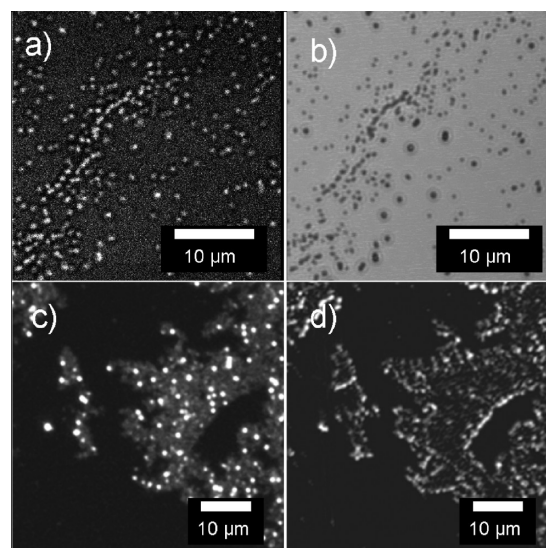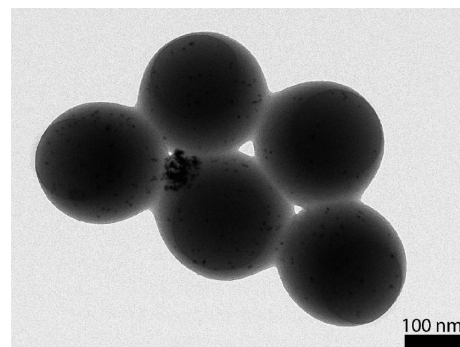
Figure 4(a)) appears at longer wavelengths than the luminescence which is collected from the darker areas (spot 3 in Figure 4(a)). A red shift of this sort indicates Förster resonance energy transfer (FRET) between the QDs.[20-23] Because FRET only appears when particles are in close proximity, the weak and short wavelength emission of the main area observed in Figure 4(a) can be attributed to homogeneously dispersed QDs in the microspheres. The observed bright spots, emitting light at longer wavelengths, can be therefore assigned to the agglomerates observed in the TEM-images (Figure 3).

Amount and Distribution of the QDs in the c-PMCs. If no agglomerates are identified, the typical loading of the c-PMCs with QDs can be estimated form the TEM-images (Figure 3; Figure 5). For doped c-PMCs 2% the number of QDs observed lies in the range of about 70 QDs per c-PMC, whereas for c-PMCs 1% typically about

(20) Förster, T. *Modern Quantum Chemistry*; Academic Press: New York, **1965**; Vol. *III*.
(21) Kagan, C. R.; Murray, C. B.; Bawendi, M. G. *Phys. Rev. B* **1996**, *54*, 8633.
(22) Muller, F.; Gotzinger, S.; Gaponik, N.; Weller, H.; Mlynek, J.; Benson, O. *J. Phys. Chem. B* **2004**, *108*, 14527.
(23) Poznyak, S. K.; Osipovich, N. P.; Shavel, A.; Talapin, D. V.; Gao, M. Y.; Eychmuller, A.; Gaponik, N. *J. Phys. Chem. B* **2005**, *109*, 1094.
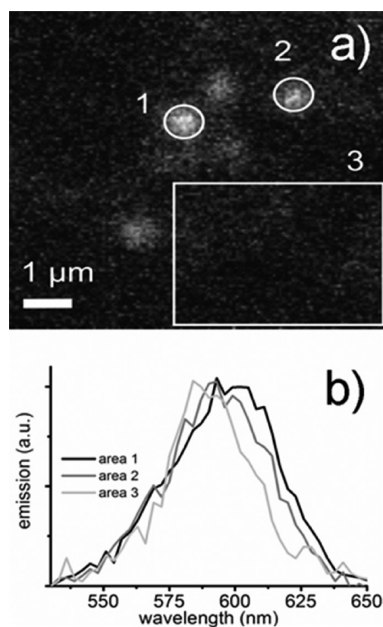
Figure 4. (a) Confocal microscopy fluorescence images of a monolayer of doped c-PCMs 2% and (b) emission spectra of different areas of this monolayer labeled in Figure 4(a).
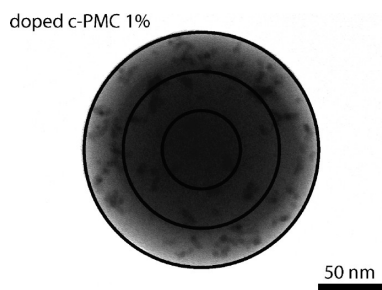

Figure 5. Distribution of QDs in a doped c-PMC 1%.

200 QDs were observed. Taking the size of the c-PMCs of about 320 nm into account this yields a loading factor of $\sim$4100 QDs/μm^3 polymer in the case of c-PMCs 2% and about 11 000 QDs/μm^3 for c-PMCs 1%. For infiltrated c-PMCs 1% with a diameter of 1.2 μm, doped by an similar procedure, Han et al. reported a doping level between 40 000 and 50 000 QDs per c-PMC.[2] This corresponds to a loading factor of between 36 000 and 45 000 QDs/μm^3 polymer. This shows that the doping level reported here is lower by a factor of 3$-$4 in comparison with the procedure reported by Han et al., but it is still in the same order of magnitude.

From TEM-images and the comparison of confocal microscopy and confocal fluorescence microscopy images it appears, that the QDs are linked to the c-PMCs but it can′t be directly concluded from these observations that the QDs are incorporated into the c-PMCs (Figures 2, 3, and 5). To get information of the distribution of the single QDs in the doped c-PMCs, TEM-images of doped c-PMCs were segmented in certain areas (Figure 5), and the number of QDs in these areas was determined. Two marginal cases were assumed: (1) Assuming a random distribution of the QDs in the volume of the c-PMCs, the fraction of the QDs determined in a certain area of the TEM-image is proportional to the volume fraction of the c-PMC represented in this area of the TEM-image; (2) Assuming a random distribution of the QDs on the surface of the c-PMCs, the fraction of the QDs determined in a certain area in the TEM-image is proportional to the surface area fraction represented in this area of the TEM-image.

The fraction of QDs observed in the segments for differently strong cross-linked c-PMCs are given in Table 1 (for the particular types of c-PMCs a statistically sufficient number of c-PMCs was investigated bringing the total number of QDs above 200). The values determined for the particular c-PMCs are between the values of the above outlined marginal cases. This indicates that the QDs are typically incorporated into the c-PMCs, but predominantly closer to the surface. This observation is reasonable taking into account an infiltration mechanism, where the QDs have to diffuse in the c-PMCs.

It is noted that in the number of QDs determined in the inner circle for doped c-PMCs 1% is surprisingly low. This might be explained by the limitations of the experiment: the inner circle also represents the area where the electron beam has to pass the longest distance trough the c-PMC during the TEM-measurement. Therefore it was difficult for this particular sample to determine the QDs in the inner circle. However, for these samples it was still easily possible to determine the number of particles in the middle ring (cf. Figure 5, Table 1). The ratio of the middle and outer ring gives here for c-PMCs 1% a value of 1.7, which is in between the ratios of the marginal cases of 1.2 (for a homogeneous distribution in the volume) and 2.7 (homogeneous distribution on the surface) and comparable with the ratio observed for a c-PMCs 2% of 1.9. Therefore it can be concluded, that the conclusion made is also valid for c-PMCs 1%.

Morphology of c-PMCs after Doping. For different applications, like for the formation of artificial opals, it is crucial that the shape and the morphology of the c-PMC samples are maintained also after doping.
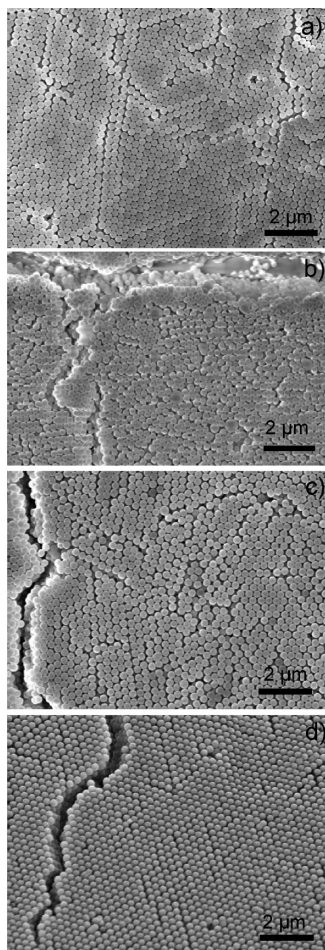
In Figure 6 SEM-images of thin opaline films made from doped and from the corresponding non doped c-PMCs are shown. The non doped c-PMCs form highly ordered opaline structures, proving a sharp size distribution of the c-PMCs (Figure 6(a) and (c)). In the case of QD doped c-PMCs 1% the structure is strongly disordered, and no long-range periodicity can be observed. This disorder is caused by larger copolymer particles (Figure 6(b)). It can be assumed, that these larger particles form due to agglomeration of the c-PMCs during the incorporation procedure, as is observed also for other incorporation procedures by swelling of c-PMCs.[24] However, in the case of the stronger cross-linked spheres (c-PMCs 2%) highly ordered opals can be obtained also after doping (Figure 6(d)). Only very few, mainly binary agglomerates of c-PMCs can be observed, which are typically almost perfectly embedded in the crystal structure.

Photonic Properties of Opaline Films Out of QD Doped c-PMCs. In Figure 7(a)$-$(d) reflection spectra of opaline films of the bare and of the corresponding QD doped

(24) Lange, B.; Zentel, R.; Ober, C.; Marder, S. *Chem. Mater*. **2004**, *16*, 5286.

Table 1. Observed Distribution of QDs in TEM-Images of c-PMCs and the Expected Values for a Homogenous Distribution of the QDs on the Surface and in the Volume of the c-PMCs

area in TEM-image	volume represented by particular area in TEM-image	surface area represented by particular area in TEM-image	doped c-PMCs 1%	doped c-PMCs 2%
inner circle	15.7%	5.7%	5%	12%
middle ring	42.9%	25.5%	36%	30%
outer ring	41.4%	68.8%	60%	57%

Figure 6. SEM images of artificial opals made from (a) c-PMCs 1%, (b) doped c-PMCs 1%, (c) c-PMCs 2%, and (d) doped c-PMCs 2%.

c-PMCs are shown. Both films manufactured from bare c-PMCs show sharp reflection lines for the first photonic band gap at wavelengths of about 625 nm and about 650 nm for c-PMCs 1% and c-PMCs 2%, respectively (Figure 7(a) and (b)). For opaline films made from doped c-PMCs 1% a weakly distinct reflection feature with a small intensity is observed (Figure 7(c)). For doped c-PMCs 2%, like in the case of the non doped c-PMCs a distinct and strong reflection line is observed at a wavelength of about 650 nm. These results are in agreement with the investigations by SEM (cf. Figure 6), where highly ordered opaline films were observed for the c-PMCs 2%, while the arrangement of the polymer spheres is strongly disturbed in the case of c-PMCs 1%.

Further it is noted, that the reflection intensity of the doped c-PMCs 2% is significantly higher than those of the nondoped ones (Figure 7(b) and (d)). This phenomenon can be explained by the superior order of the opal
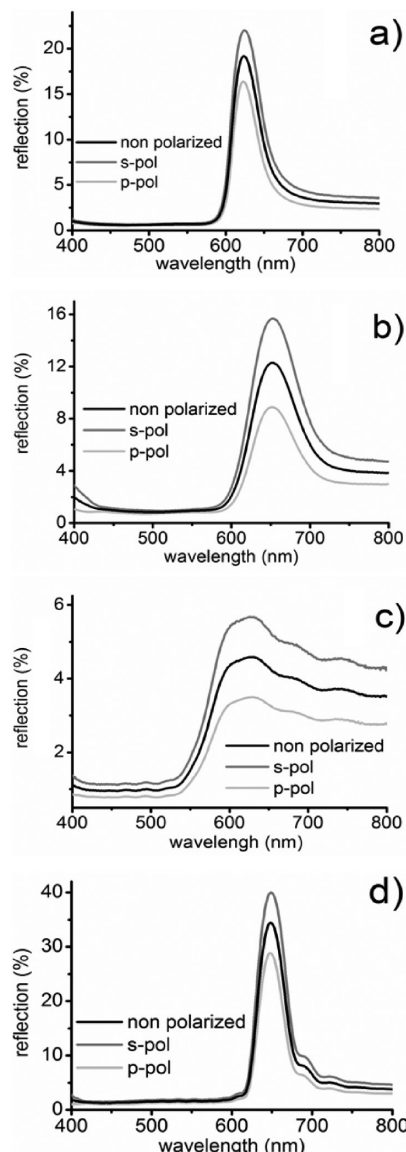
Figure 7. Reflection spectra of artificial opals made from (a) c-PMCs 1%, (b) c-PMCs 2%, (c) doped c-PMCs 1%, and (d) doped c-PMCs 2%. S-pol and p-pol: linear polarization perpendicular and parallel to the plane of incidence, respectively.

of the doped c-PMCs in comparison to the opal of the nondoped c-PMCs (observed in the SEM-images), in spite of the small agglomerates in the doped sample (Figure 6(c) and (d)). This better packing might have its origin in the additional purification steps, and therefore can be simply seen as an indication for the high purity of the suspension of the doped c-PMCs.

Angular Dependent Emission of Artificial Opals Build of QD Doped c-PMCs. To investigate the effect of the
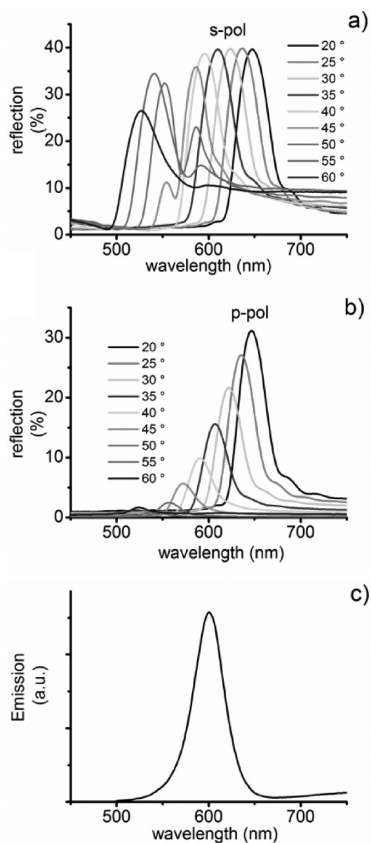
Figure 8. Angular dependent reflection spectra of artificial opals made from c-PMCs 2%, (a) s-pol, (b) p-pol, and (c) emission spectrum of a suspension of c-PMCs 2% in water.

photonic band structure on the emission properties in dependence of the angle, a more detailed understanding of the photonic properties of the particular opal is necessary. In Figure 8(a) and (b) specular reflectance spectra of an opal composed of doped c-PMCs 2% are shown. It appears that the intensity of the photonic bandgap reflection for s-pol is higher over the whole angular range. Further, starting from angles of 45°, beside the reflection of the 111-lattice plane also the reflection of the 200-latrice plane of the fcc−lattice appears for s-pol light, oppositely p-pol light. This is expected from literature:

It is described, that the bandgap reflection of the 200-lattice plane is much weaker for p-pol light and that it appears at longer wavelengths in comparison to s-pol light, so that we do not observe for p-pol separate reflection maxima like in the case of s-pol.[25] Further the width of the reflection of the 111-lattice plane is broader for s-pol than for p-pol, yielding a shorter Bragg-attenuation length L_B, and finally leading to a stronger reflection for s-pol light.[3,26]

$$L_B = \frac{E_B}{\Delta E} \frac{\pi}{2 d_{xyz}}$$

with E_B, the energy at which the transmission minimum due to the photonic band gap is observed, ΔE, the energy full

(25) Galisteo-López, J. F.; Palacios-Lidón, E.; Castillo-Martínez, E.; López, C. *Phys. Rev. B* **2003**, *68*, 115109.
(26) Galisteo-López, J. F.; López--Tejera, F.; Rubio, S.; López, C.; Sánchez-Dehesa, J. *Appl. Phys. Lett.* **2003**, *82*, 4068.
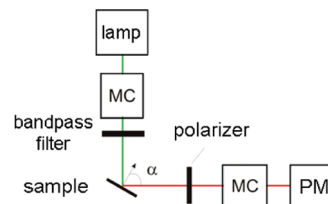
Figure 9. Setup for the determination of the emission spectra of opaline samples. MC: monochromator, PM: photo multiplier.
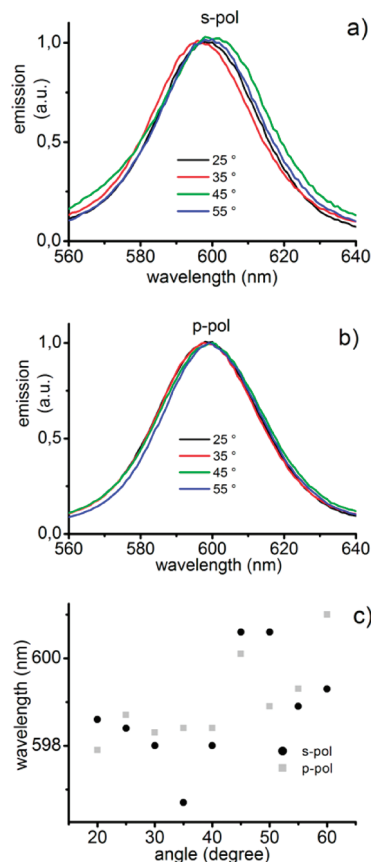

Figure 10. Emission spectra of an opal of doped c-PMCs 2% a different angles (a) s-pol, (b) p-pol. (c) Wavelengths of the emission maxima at different angles.

width at half minimum of the transmission minimum and d_{xyz}, the particular lattice spacing.

The comparison with the emission spectrum of a suspension of the doped c-PMCs in water shows, that an overlap of the emission band of the QDs and the photonic band gap at s-pol and p-pol has to be expected for emission angles (angle between the normal of the opaline film and the emitted beam) between 35° and 40°.

To investigate this, the luminescence of an opal of c-PMCs 2% was measured in front face geometry (Figure 9). The normalized emission spectra at the particular angles gained by means of these measurements are shown in Figure 10(a) and (b). As a function of the angle only small changes of the peak wavelength are observed in both cases. However it still turns out that the change of the emission wavelength is stronger when s-pol light is investigated, being in agreement with the observations from the absorption spectra. In Figure 10(c) the position of the emission maxima in relation

to the angle is shown. For s-pol light a clear minimum at 35°, and a maximum between 45° and 50° of the emission wavelength is observed. For p-pol light the behavior is less clear and only a maximum of the emission wavelength is observed at 45°. For both measurements an increasing emission wavelength is observed at larger angles. Although the effects are small, they are still in agreement with the observations from the reflection spectra. We see a change of the emission wavelength exactly at the angles, at which the reflection, caused by the photonic band gap, passes the emission line. Furthermore, this effect is stronger investigating s-pol light.

An explanation requires a look at the measurement geometry:

The opal observed here possessed a thickness of about 17 layers, which corresponds to about 4.8 μm (diameter spheres according dynamic light scattering 344 nm, assuming a lattice spacing along the 111-axis of $d_{111} = (2/3)^{1/2}d$, with d the diameter of the spheres).

Taking into account, that the typical Bragg-attenuation length for opals out of PMCs is in the range of 2 μm,[3] it can be assumed that the emission of the layers of the opals closer to the front face is almost unaltered. Further, the excitation beam enters from the frontside inferring

that the main intensity of emission also stems from the c-PMCs close to the front side which is only weakly affected by the photonic band structure.

This assumption is in agreement with work by Fleischhaker et al.,[14] where it was shown, that light emitted from an opal is only weakly attenuated in front face geometry as opposed to experiments performed with exciation and detection on opposite sides of the opals.[27,28]

Conclusions

In this work we show a facile strategy how PMMA/PDVB-copolymer microspheres which are initially suspended in water can be doped with QDs in an organic solvent mixture and be finally gained in water. We proof, that the QDs are present within the polymer spheres. Further we show that the aqueous suspensions of the doped PMMA/PDVB-copolymer microspheres can be used to prepare high quality artificial opals. Further we show the interaction of the emission of the QDs with the photonic band structure. Therefore we assume that the presented material bares potential with respect of bioimaging and photonic crystal applications.

(27) Gaponenko, S. V.; Kapitonov, A. M.; Bogomolov, V. N.; Prokofiev, A. V.; Eychmüller, A.; Rogach, A. L. *JETP Lett.* **1998**, *68*, 142.
(28) Fleischhaker, F.; Arsenault, A. C.; Schmidtke, J.; Ozin, G. A.; Zentel, R. *Chem. Mater.* **2006**, *18*, 5640.